

# Postnatal environmental enrichment enhances memory through distinct neural mechanisms in healthy and trisomic female mice



Maria Alemany-González <sup>a</sup>, Marta Vilademunt <sup>a</sup>, Thomas Gener <sup>a,b,c</sup>, M. Victoria Puig <sup>a,b,c,\*</sup>

<sup>a</sup> Integrative Pharmacology and Systems Neuroscience, Hospital del Mar Medical Research Institute, Barcelona Biomedical Research Park, 08003 Barcelona, Spain

<sup>b</sup> Catalan Institute of Nanoscience and Nanotechnology (ICN2), the Barcelona Institute of Science and Technology (BIST), Campus UAB, Bellaterra, 08193 Barcelona, Spain

<sup>c</sup> Institut de Neurociències, Universitat Autònoma de Barcelona, 08193 Bellaterra, Barcelona, Spain

## ARTICLE INFO

### Keywords:

Intellectual disability  
Down syndrome  
Prefrontal cortex  
Hippocampus  
Functional connectivity  
Cognitive stimulation  
Neural synchrony  
Ts65Dn Genetic mouse model  
Memory impairment  
REM sleep

## ABSTRACT

Stimulating lifestyles have powerful effects on cognitive abilities, especially when they are experienced early in life. Cognitive therapies are widely used to improve cognitive impairment due to intellectual disability, aging, and neurodegeneration, however the underlying neural mechanisms are poorly understood. We investigated the neural correlates of memory amelioration produced by postnatal environmental enrichment (EE) in diploid mice and the Ts65Dn mouse model of Down syndrome (trisomy 21). We recorded neural activities in brain structures key for memory processing, the hippocampus and the prefrontal cortex, during rest, sleep and memory performance in mice reared in non-enriched or enriched environments. Enriched wild-type animals exhibited enhanced neural synchrony in the hippocampus across different brain states (increased gamma oscillations, theta-gamma coupling, sleep ripples). Trisomic females showed increased theta and gamma rhythms in the hippocampus and prefrontal cortex across different brain states along with enlarged ripples and disrupted circuit gamma signals that were associated with memory deficits. These pathological activities were attenuated in their trisomic EE-reared peers. Our results suggest distinct neural mechanisms for the generation and rescue of healthy and pathological brain synchrony, respectively, by EE and put forward hippocampal-prefrontal hypersynchrony and miscommunication as major targets underlying the beneficial effects of EE in intellectual disability.

## 1. Introduction

A rich social, physical, and cognitive lifestyle has powerful effects on cognitive abilities and brain function. Cognitive training programs are the main nonpharmaceutical interventions used to ameliorate cognitive decline due to aging or neurodegenerative diseases (Livingston et al., 2017) and are the only therapy currently available for people with Down syndrome (DS, trisomy 21). In DS subjects, cognitive therapy improves executive functions and adaptive functionality (de la Torre et al., 2016; Karaaslan and Mahoney, 2013; Martínez Cué and Dierssen, 2020) via a neuroplastic reorganization of the brain (Anagnostopoulou et al., 2021). DS brains display increased brain synchrony as assessed by EEG, MEG and fMRI (Anderson et al., 2013; Figueiroa-Jimenez et al., 2021; Pujol et al., 2015; Ramírez-Torano et al., 2021; Velikova et al., 2011), however the exact neural mechanisms involved in the cognitive training-

dependent brain reorganization have not been elucidated.

Environmental enrichment (EE) mimics a stimulating lifestyle in laboratory animals and has demonstrated beneficial effects on various aspects of brain structure and function, including cognition. It promotes dendritic branching and synaptic plasticity in the hippocampus (HPC) and the prefrontal cortex (PFC; Hirase and Shinohara, 2014; van Praag et al., 2000), two brain regions crucial for learning and memory, and improves cognitive performance in several tasks such as learning, working memory, and recognition memory (Brenes et al., 2016; Leger et al., 2015; Mesa-Gresa et al., 2013; Wang et al., 2020). Studies conducted in anesthetized rodents report that animals reared in enriched environments present enhanced gamma rhythms within hippocampal microcircuits (Hirase and Shinohara, 2014; Shinohara et al., 2013; Tanaka et al., 2017; van Praag et al., 2000). However, no studies have yet investigated how experience modulates long-range connectivity

**Abbreviations:** Down syndrome, DS; environmental enrichment, EE; prefrontal cortex, PFC; hippocampus, HPC; trisomy, TS; discrimination index, DI; rapid eye movement sleep, REM sleep.

\* Corresponding author at: Catalan Institute of Nanoscience and Nanotechnology (ICN2), Barcelona, Spain.

E-mail address: [victoria.puig@icn2.cat](mailto:victoria.puig@icn2.cat) (M.V. Puig).

<https://doi.org/10.1016/j.nbd.2022.105841>

Received 9 June 2022; Received in revised form 12 August 2022; Accepted 15 August 2022

Available online 18 August 2022

0969-9961/© 2022 The Authors. Published by Elsevier Inc. This is an open access article under the CC BY-NC-ND license (<http://creativecommons.org/licenses/by-nc-nd/4.0/>).

during wakefulness and natural sleep.

EE has also been found to attenuate molecular, cellular, and behavioral deficits in animal models of numerous neurological and psychiatric disorders (Nithianantharajah and Hannan, 2006) and it exerts profound changes in the brains and behaviors of DS animal models. The Ts65Dn partial trisomic DS model, with triplication of ~90 genes ortholog for genes located in human chromosome 21, exhibits behavioral, cellular, and molecular phenotypes relevant for DS. Overexpression of genes disrupts neurogenesis and synaptic plasticity in Ts65Dn mice, simplifies dendritic architecture, and imbalances excitation–inhibition that leads to a general overinhibition (Belichenko et al., 2007; Cramer and Galdzicki, 2012; Kleschevnikov et al., 2004; Ruiz-Mejias, 2019). EE decreases inhibition and ameliorates dendritic complexity, synaptic plasticity and cognitive performance in DS mice both during development and adulthood (Begenisic et al., 2015, 2011; Martínez-Cué et al., 2005, 2002; Pons-espinal et al., 2013).

Here we aimed to unravel the neural substrates of memory amelioration produced by EE experienced early in life in diploid healthy mice and trisomic DS mice. We used Ts65Dn females because they are more sensitive to EE than Ts65Dn males (Martínez-Cué et al., 2002). In consonance with the increased brain synchrony reported in clinical studies, we have recently demonstrated hypersynchronous neural activities in hippocampal-prefrontal pathways of Ts65Dn males that are partially rescued by green tea extracts containing epigallocatechin-3-gallate (EGCG) (Alemany-González et al., 2020; Puig et al., 2020). This study allowed us to assess abnormal neural activities in male and female trisomic subjects and compare the actions of EGCG and EE on the same circuits.

## 2. Materials and methods

### 2.1. Animals

Ts65Dn female mice ( $n = 13$ ) and their wild-type littermates ( $n = 12$ ) were obtained by breeding B6EiC4Sn.BLiA-Ts(1716)65Dn/DnJ females with C57BL/6 × 6JOlaHsd (B6C3F1/OlaHsd) hybrid males. The parental generation was obtained from the Jackson Laboratory (Bar Harbor, ME) and a colony was generated and maintained at the Barcelona Biomedical Research Park (PRBB) Animal Facility. Mice were genotyped and ~25% of the offspring showed trisomy. Aged-matched diploid littermates served as controls. Animals were 2 to 3 months old at the start of all experiments and weighed between 20 and 30 g. All procedures were conducted in compliance with EU directive 2010/63/EU and Spanish guidelines (Laws 32/2007, 6/2013 and Real Decreto 53/2013) and were authorized by the Barcelona Biomedical Research Park (PRBB) Animal Research Ethics Committee and the local government.

### 2.2. Environmental enrichment protocol

Female mice were housed in non-enriched or enriched conditions for 7 weeks after weaning. The non-enriched environment consisted in standard Plexiglas cages (37 × 16.5 × 13.5 cm) where mice were housed in groups of 2 to 3 individuals. Mice reared in enriched conditions were housed in groups of 5 to 7 individuals in large two-level cages (55 × 80 × 50 cm) with plastic toys that were replaced every three days. This enriched environment promoted sociability, physical exercise, and cognitive development. Diploid and trisomic mice were housed together in both rearing conditions. Typically, one trisomic mouse was housed with one or two diploid mice in the non-enriched environment. In the enriched environment, two trisomic mice were housed with 2 to 4 diploid mice. All the trisomic mice and the same number of diploid cagemates underwent surgery for chronic electrode implantation during the first week after completing the seven-week rearing period. The rest of the diploid animals were euthanized. The surgery was followed by one week of post-surgical recovery (Fig. 1A). All the mice were housed

individually from the day of the surgery until the end of the experiment to prevent the implants from being damaged by other cage mates. Mice in the enriched group had toys in their cages that were replaced every three days until the end of the experiment.

### 2.3. Stereotaxic surgeries

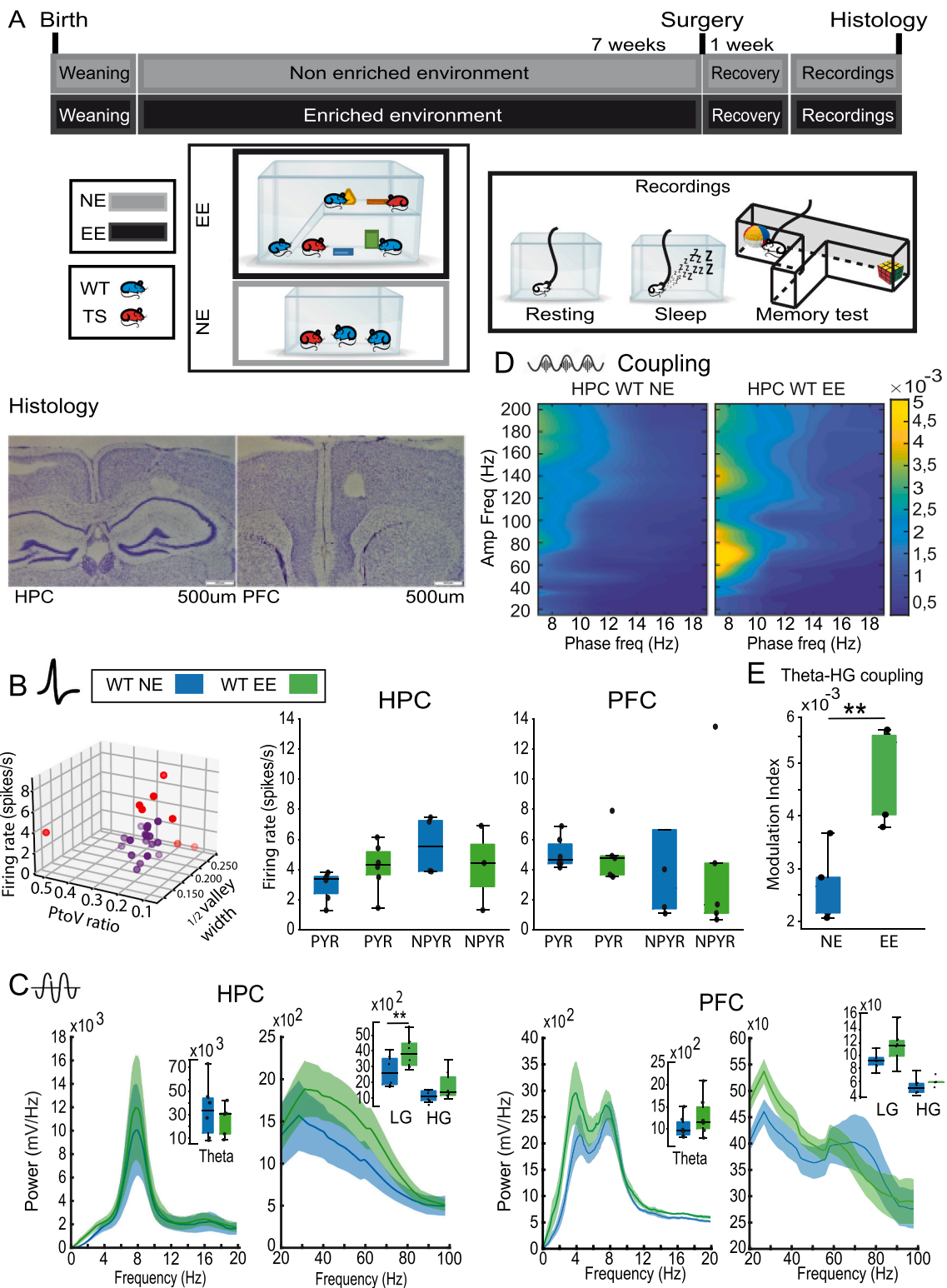
Mice were anesthetized with a mixture of ketamine/xylazine (ketamine: Imalgene 1000, Distrijet SA; xylazine: X1251-1G, Sigma-Aldrich) and placed in a stereotaxic apparatus. Anesthesia was maintained with continuous 0.5–4% isoflurane (Zoetis Spain, S.L.). Small craniotomies were drilled above the medial PFC and the HPC. Five micro-screws were screwed into the skull to stabilize the implant, and the one on top of the cerebellum was used as a general ground. Three tungsten electrodes, one stereotrode and one single electrode, were implanted in the PFC and three more were implanted in the HPC. The electrodes were positioned stereotactically in the prelimbic PFC (AP: 1.5, 2.1 mm; ML: ± 0.6, 0.25 mm; DV: −1.7 mm from bregma) and in the CA1 area of the HPC (AP: −1.8, −2.5 mm; ML: −1.3, −2.3 mm; DV: −1.15, −1.25 mm). In addition, three reference electrodes were implanted in corpus callosum and lateral ventricles (AP: 1, 0.2, −1; ML: 1, 0.8, 1.7; DV: −1.25, −1.4, −1.5, respectively). The electrodes were made by twisting a strand of tungsten wire 25 μm wide (Advent, UK), had impedances that ranged from 100 to 400 kΩ at the time of implantation and were implanted unilaterally with dental cement. Electrode wires were pinned to an adaptor to facilitate their connection to the recording system. After surgery, animals were allowed to recover during at least one week in which they were extensively monitored and received both analgesia and anti-inflammatory treatments. Additionally, animals were handled and familiarized with the implant connected to the recording cable. After the experiments ended, a mild electrical current (100 Hz, 0.1 mA, 2 s) was applied to the electrodes to mark the placement of electrode tips, which were later confirmed histologically by staining the brain slices with Cresyl violet (Sigma-Aldrich). Electrodes with tips outside the targeted areas (CA1 and prelimbic mPFC) were discarded for data analyses.

### 2.4. Behavioral and neurophysiological characterization

We recorded single-unit activity (SUA) and local field potentials (LFPs) in freely moving mice with the multi-channel Open Ephys system at a sampling rate of 30 kHz with Intan RHD2132 amplifiers equipped with an accelerometer. We used the accelerometer's signals in the X, Y and Z axis to monitor general mobility of mice. We found that the variance of the instantaneous acceleration module (Acc), that quantifies the variation of movement across the three spatial dimensions, was maximal during exploration and decreased as the animals were in quiet alertness and natural sleep (Alemany-González et al., 2020; Gener et al., 2019). More specifically, raw X, Y and Z signals were first downsampled to 1 kHz, then we calculated the instantaneous module (root square [ $X^2, Y^2, Z^2$ ]) from which we measured the variance. In addition, recorded signals from each electrode were filtered offline to extract SUA and LFPs. SUA was estimated by first subtracting the raw signal from each electrode with the signal from a nearby referencing electrode to remove artifacts related to the animal's movement. Next, referenced signals were filtered between 450 and 6000 Hz and the spikes from individual neurons were sorted using principal component analysis with Offline Sorter v4 (Plexon Inc). To obtain LFPs, signals were downsampled to 1 kHz, detrended and notch-filtered to remove noise line artifacts (50 Hz and its harmonics) with custom-written scripts in Python. Signals were then imported into MATLAB. The frequency bands considered for the band-specific analyses included theta (8–12 Hz), low gamma (30–50 Hz), high gamma (50–80 Hz), and higher frequencies (100 to 150 Hz) when appropriate.

#### 2.4.1. Quiet wakefulness, NREM and REM sleep

Recordings during quiet wakefulness were performed in an empty



(caption on next page)

**Fig. 1.** EE enhances pyramidal activity and gamma synchrony in the HPC of healthy females during rest. A: Experimental timeline. After weaning, mice were reared in enriched or non-enriched environments for 7 weeks. Typically, one trisomic mouse was housed with one or two diploid mice in the non-enriched environment while two trisomic mice were housed with 2 to 4 diploid mice in the enriched environment. All the trisomic mice and the same number of diploid cage mates underwent surgery for chronic electrode implantation in the HPC and the mPFC during the first week after completing the seven-week rearing period. The surgery was followed by one week of post-surgical recovery after which we recorded neural activities during resting periods, sleep, and memory performance. The results for the diploid groups are shown in Figs. 1 to 3 and those of the trisomic groups are shown in Figs. 4 to 6. Also shown are representative examples of histological validations in CA1 and prelimbic PFC. Note the small lesions caused by low-intensity electrical stimulations, which were used to mark the tips of the electrodes after the last recording session. B: Neurons were classified based on three electrophysiological properties: peak-to-valley ratio and half-valley width of the action potentials, and the firing rate (Kim et al., 2016; Alemany-González et al., 2020). Purple dots denote putative pyramidal neurons (wide spiking), and red dots represent unclassified putative non-pyramidal neurons. Shown is a representative 3D plot including all the neurons recorded in the HPC in the wild-type NE group ( $n = 6$  mice). Also shown are the mean firing rates per animal of presumed pyramidal and non-pyramidal neurons in HPC and PFC. Number of pyramidal neurons isolated in each brain region in wild-type NE and EE mice: [HPC]  $n = 23, 23$  neurons; [PFC]  $n = 18, 26$  neurons. Non-pyramidal neurons: [HPC]  $n = 13, 11$  neurons; [PFC]  $n = 12, 11$  neurons. C: Power spectra of signals in HPC and PFC during rest. D: Co-modulation maps of cross-frequency coupling in the HPC. Color scale indicates modulation index (MI) in all figs. E: Quantification of theta-high gamma MI in the HPC. Data are represented as mean  $\pm$  SEM. \* $P \leq 0.05$ , \*\* $P \leq 0.01$ . (For interpretation of the references to color in this figure legend, the reader is referred to the web version of this article.)

cage for 10 min. Briefly, low mobility was determined by a defined threshold in the output of the accelerometer signals and normal movement was defined as above that threshold. The animals typically rested for brief periods between 2 and 10 consecutive seconds. Recordings during natural sleep were implemented following the familiarization phase of the NOR task to better capture neural signals related to memory consolidation (Fig. 2A). Accelerometer measures and LFP signals from the PFC and the HPC were used to score epochs of REM and NREM sleep. NREM sleep was behaviorally defined as presenting immobility (low variations of the accelerometer) and large amplitude slow oscillations (1–4 Hz) in the PFC and HPC. Only periods of deep NREM sleep prior to REM episodes were considered for analysis. REM epochs were defined as immobility and prominent hippocampal theta rhythms. Analyses of LFPs signals during quiet wakefulness and natural sleep were performed averaging neural signals over discrete epochs of different duration (one continuous epoch per experiment; quiet wakefulness: 3 min; NREM sleep: 1 min; REM sleep: 10 s) that were chosen based on the stability of the brain state (McShane et al., 2012).

#### 2.4.2. Novel object recognition test

We tested recognition memory using a well-established task that relies on mice' innate instinct to explore novel objects in the environment (McShane et al., 2012). We used a custom-designed T-maze made of aluminum with wider and higher arms than the standard mazes (8 cm wide  $\times$  30 cm long  $\times$  20 high). The maze was shielded and grounded for electrophysiological recordings and was placed on an aluminum platform. The T shape of the maze also favored more visits to the objects by the mice. The novel-familiar object pairs were previously validated as in Gulinello et al., 2018. The arm of the maze where the novel object was placed was randomly chosen across experiments. The test was implemented in three phases of 10 min each: habituation and familiarization during the first day and long-term memory test 24 h after familiarization. Mice were first habituated to an empty maze. Five minutes later, mice were placed again in the maze where they could explore two identical objects located at the end of the two lateral arms. Twenty-four hours later, in the test phase, mice were presented with one familiar and one novel object. Each session was videotaped via a video camera located on top of the maze. Any investigative behavior of objects, including head orientation towards the objects or sniffing at a distance below or equal to 2 cm or when the mice touched the objects with the nose, was considered object exploration. Exploratory events were identified online by looking at the video using a custom-designed joystick with a right and left button that were pressed continuously during the time of explorations. Button presses were automatically aligned to the electrophysiological file by sending TTL pulses to the acquisition system so that two more event channels were added to the recording files. Object recognition memory was defined by the discrimination index (DI) for the novel object using the difference in exploration time for the familiar object divided by the total amount of exploration of both objects (DI = [time of novel object exploration-time

of familiar object exploration]/total exploration time). DIs varied between +1 and -1, where a positive score indicated more time spent with the novel object, a negative score indicated more time spent with the familiar object, and a zero score indicated a null preference (Leger et al., 2013). LFP measures associated with memory acquisition and retrieval were obtained by averaging one-second non-overlapping windows triggered by the button presses on the joystick. Epochs that contained electrical artifacts were discarded from the analyses. Each one-second window was only considered if the mouse explored the object for at least 600 ms. This allowed us to include many visits that were particularly short while also granting a good estimation of power at low frequencies. Memory retrieval was investigated in the 24 h memory test during the visits to familiar objects. Memory acquisition and novelty seeking, which cannot be disentangled in this task, were investigated in the 24 h memory test during the visits to novel objects. As in our previous study (Alemany-González et al., 2020), we found that these criteria provided the most robust results.

## 2.5. Data analyses

### 2.5.1. Power spectral analysis

We used the multitaper fast Fourier transform method (time frequency bandwidth; TW = 5 and K = 9 tapers; 1–100 Hz range; non-overlapping sliding window of 5 s for power spectra, 2 s for spectrograms, 1 s for object explorations) with the Chronux toolbox in MATLAB (Bokil et al., 2010).

### 2.5.2. Phase-amplitude modulation index

To quantify the intensity of phase-amplitude coupling we used the modulation index (MI) as described in (Tort et al., 2010). First, low frequency (delta and theta) phases were divided into 18° bins and gamma (low, high gamma and high frequency oscillations-HFO) amplitude was calculated for each phase bin. MI measures the divergence of the phase-amplitude distribution and is higher as it is further away from the uniform distribution. To choose specific frequency bands pairs for the MI quantification we represented overall MI in a two-dimensional pseudocolor comodulation map. A warmer color indicates coupling between the phase of the low frequency band (x axis) and the amplitude of the high frequency band (y axis) while blue depicts absence of coupling.

### 2.5.3. Phase slope index (PSI)

To estimate the flow of information between neural signals of the PFC and HPC, we used the Phase Slope Index as in Nolte et al., 2008 with the data2psi.m function. PSI is a robust measure based on the conceptual temporal argument supporting that the driver is earlier than the recipient and contains information about the future of the recipient. It quantifies the consistency of the direction of the change in the phase difference across frequencies. Positive slope reflects an HPC-to-PFC (HPC  $\rightarrow$  PFC) flow of information in a specific frequency range while a

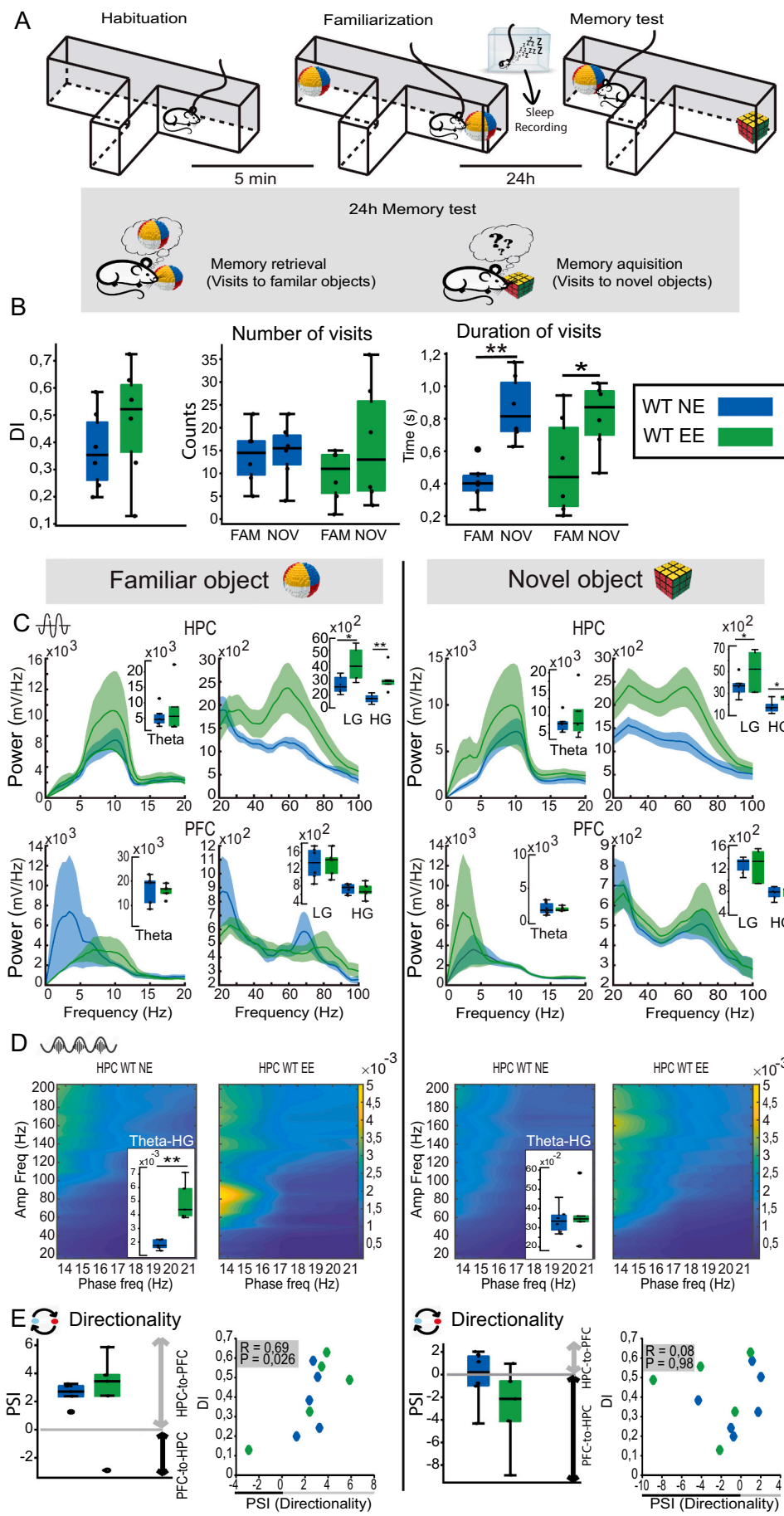


**Fig. 2.** EE entrains hippocampal gamma oscillations and hippocampal-prefrontal gamma connectivity in healthy mice during memory retrieval. **A:** The novel object recognition task. **B:** Discrimination indices (DIs) and number of visits to familiar and novel objects were similar between rearing groups. Visits to novel objects were longer than to familiar objects in both groups. **C:** Power spectra of signals in HPC and PFC. Quantifications of relevant bands are also shown. During the visits to familiar objects EE mice exhibited enhanced low/high gamma power in the HPC (mixed ANOVA, region  $\times$  rearing interaction:  $F_{1,9} = 9.105$ ,  $14.689$ ;  $P = 0.015$ ,  $0.004$ ; HPC:  $P = 0.029$ ,  $0.007$ ; PFC:  $P = 0.99$ ,  $0.65$ ). During the visits to novel objects, low/high gamma power also tended to increase in the HPC of EE mice, but less consistently than during the visits to familiar objects ( $F_{1,9} = 3.47$ ,  $5.11$ ;  $P = 0.09$ ,  $0.05$ ). **D:** Co-modulation maps of cross-frequency coupling in the HPC and corresponding quantification of theta-high gamma MI. **E:** HPC-to-PFC directionality (PSI) at low gamma frequencies and corresponding correlations with DIs.

negative slope reflects the opposite directionality of signals.

#### 2.5.4. Analysis of ripples during NREM sleep

Raw signals were downsampled to 1.25 kHz and bandpass filtered between 100 and 600 Hz. Sharp-wave ripple events were detected by thresholding ( $>3$  SDs) the filtered signals using ripple detection scripts from M. Valero (Valero et al., 2017). Time-frequency analysis of ripples was calculated using multitaper spectral estimation and frequency resolution of 10 Hz in the 100–600 Hz range.

#### 2.5.5. Analyses of entropy

To quantify the level of frequency dispersion (and consequently the level of synchronization in the neuronal activity), we performed analysis of the spectral entropy (based on Shannon entropy) of the LFP (30–150 Hz), where a narrower power distribution results in lower entropy values, and a large power distribution results in higher entropy values, with no dependency on the LFP frequency (Valero et al., 2017).

#### 2.6. Statistical analysis

We used unpaired *t*-tests to compare behavioral measures between genotypes. Paired *t*-tests and mixed ANOVAs were used to assess the effects of environmental enrichment on power and firing rate across brain regions. Two-WAY ANOVAs were used to assess the effects of environmental enrichment on power and firing rate across genotypes. Mann-Whitney and Kruskal-Wallis non-parametric tests were used to assess the effects of enrichment on phase-amplitude coupling (PAC), entropy, and directionality of signals (PSI). We used Bonferroni correction or Tukey HSD post-hoc tests when appropriate. To identify significant correlations between neurophysiological measures and DIs, Pearson or Spearman correlations were used for parametric and non-parametric distributions, respectively. All statistical analyses were performed in MATLAB R2019a (The Mathworks, MA, USA) and the level of significance was set to  $p < 0.05$ . Results are expressed as mean ( $\pm$  SEM). SPSS and JASP 0.15 were used for statistical analyses.

### 3. Results

#### 3.1. Female mice reared in enriched environments exhibit increased gamma synchrony in the hippocampus during rest

We investigated differential neural dynamics in hippocampal-prefrontal pathways between mice reared in enriched environments (EE group) and non-enriched environments (NE group) for seven weeks after weaning. Animals reared in enriched conditions were housed in groups of 4 to 6 subjects in large cages with toys that promote physical activity. The toys were replaced every few days to keep physical and cognitive stimulation constant over weeks. Animals reared in non-enriched conditions were housed in standard cages without toys in groups of 2 or 3 individuals. Following the periods with or without enrichment, animals were implanted with electrodes in the CA1 region of the HPC and the prelimbic medial PFC. We then recorded neural activities during resting episodes, natural sleep, and memory performance. Diploid and trisomic mice were mixed in the enriched and non-enriched cages (Fig. 1A). The results for the diploid groups are shown in Figs. 1 to 3 and those of the trisomic groups are shown in Figs. 4 to 6.

We first investigated differences in the firing rate of neurons between wild type enriched and non-enriched mice during resting states. We classified neurons as putative pyramidal and non-pyramidal cells based on the shape of their action potentials and their firing pattern (Fig. 1B; Alemany-González et al., 2020; Kim et al., 2016). Around 70% and 65% of neurons recorded in the HPC and PFC, respectively, were identified as putative pyramidal cells. Presumed pyramidal neurons in the HPC of EE mice tended to fire more action potentials than in NE mice but the difference did not reach significance ( $n = 6$  mice per group; mixed ANOVA, rearing x region interaction  $F_{1,20} = 2.67$ ,  $P = 0.11$ ; EE and NE: 4.38 and

2.61 spikes/s, respectively), whereas spiking activity in the PFC was similar between groups (4.13 and 4.66, respectively). The firing rate of presumed non-pyramidal neurons was similar between rearing groups in both brain regions (Fig. 1B).

Concomitantly, low gamma power (30–50 Hz) was increased in the HPC of the enriched group (ANOVA,  $F_{1,10} = 9.739$ ,  $P = 0.011$ ; post hoc comparisons, HPC:  $P = 0.009$ , PFC:  $P = 0.11$ ; Fig. 1C). We further quantified the coupling between the phase of slow rhythms (5–20 Hz) and the amplitude of faster oscillations (20–200 Hz) in the HPC (Delgado-Sallent et al., 2021; Jensen and Colgin, 2007; Scheffer-Teixeira and Tort, 2017). Coupling was strengthened between phases from 5 to 9 cycles/s (theta) and amplitudes from 60 to 80 cycles/s (high gamma) in enriched females (Mann-Whitney test,  $P = 0.008$ ; Fig. 1D,E). Together, these results identified relevant roles for hippocampal gamma synchrony in the cellular mechanisms of EE in healthy mice during rest.

#### 3.2. Environmental enrichment entrains hippocampal gamma oscillations and hippocampal-prefrontal gamma connectivity during memory retrieval

We next investigated how enriched or non-enriched environmental stimulation early in development impacts memory performance and its neural correlates in young adulthood. We used the novel object recognition (NOR) task, a well validated memory test that relies on the mice' innate instinct to explore novel objects and depends on hippocampal-prefrontal circuits (Warburton and Brown, 2015; Alemany-González et al., 2020; Wang et al., 2021). The task was implemented in a T-maze and consisted of a habituation phase, familiarization phase, and memory test phase, each lasting ten minutes. During the habituation phase, the animals explored the maze without objects. Five minutes later, for the familiarization phase the mice were put back in the maze where two identical objects had been placed at the end of the lateral arms. Twenty-four hours later, a familiar object and a new object were placed in the maze for the memory test. We investigated the neural substrates of memory acquisition and retrieval by comparing the neural signals recorded during the visits to novel and familiar objects, respectively, during the memory test (Fig. 2A).

Discrimination indices (DIs) for novel versus familiar objects were positive for all the mice ([time visiting the novel object - time visiting the familiar object] / total exploration time; mean DI  $0.42 \pm 0.05$ ,  $n = 12$  mice); that is, mice explored novel objects more than familiar objects, indicating good recognition memory. As observed in a previous study (De Toma et al., 2019), EE mice tended to display higher DIs than NE mice ( $0.47 \pm 0.09$  vs.  $0.37 \pm 0.06$ ,  $n = 6$  mice per group), however this difference did not reach significance (unpaired *t*-test,  $P = 0.36$ ). This was likely due to ceiling effects on behavioral performance. We quantified the number of visits to each object and the mean duration of individual visits per session. Mice of the two groups visited novel objects on more occasions than familiar objects during each session (16 vs. 12 visits on average) and the visits lasted longer ( $840 \pm 58$  ms to novel objects vs.  $460 \pm 66$  ms to familiar objects; mixed ANOVA, duration x object interaction;  $F_{1,10} = 28.95$ ;  $P < 0.0005$ ; NE mice,  $P = 0.001$ ; EE mice,  $P = 0.013$ ; Fig. 2B).

Despite the modest beneficial effects of EE on memory performance, differential neural activities were detected between the two rearing groups. During the visits to familiar objects, like in resting states, EE mice exhibited enhanced low/high gamma power in the HPC (mixed ANOVA, region x rearing factors; Fig. 2C) and strengthening of theta-high gamma coupling (9–14 cycles/s with 50–80 cycles/s; Mann-Whitney test,  $P = 0.008$ ; Fig. 2D). During the visits to novel objects, low/high gamma power also tended to increase in the HPC of EE mice, but less consistently than during the visits to familiar objects (mixed ANOVA; Fig. 2C), while hippocampal theta-gamma coupling was unchanged (Mann-Whitney test,  $P > 0.05$ ; Fig. 2D).

We further detected a neural information flow (via the phase slope index or PSI; Nolte et al., 2008) at low gamma frequencies that traveled from the HPC to the PFC during the visits to familiar objects that

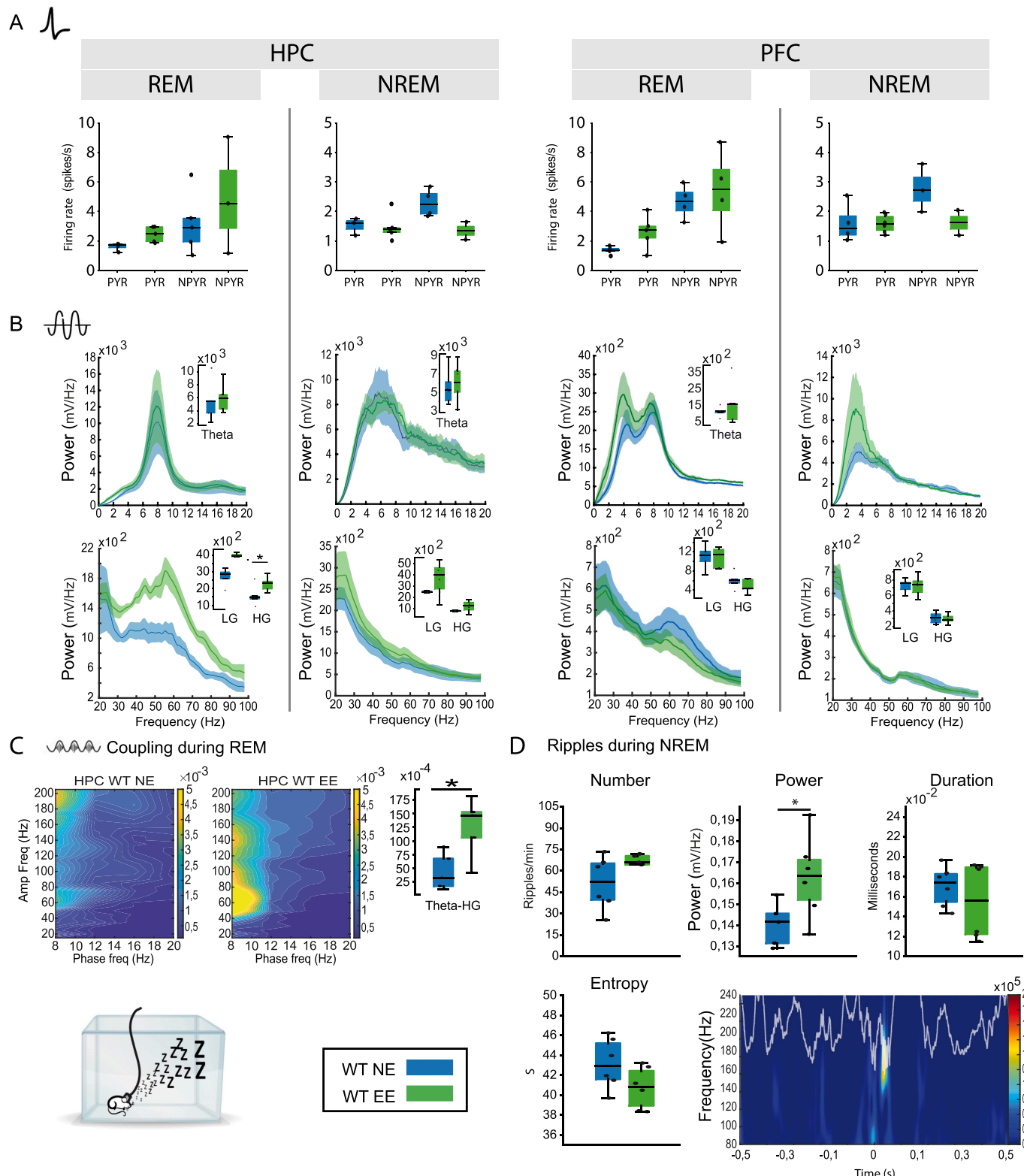


**Fig. 3.** EE enhances pyramidal activity and hippocampal gamma and ripple synchrony in healthy mice during sleep. **A:** Mean firing rates per animal in the HPC and PFC during REM and NREM sleep. Number of presumed pyramidal neurons isolated in each brain region and brain state in NE and EE wild-type mice: [HPC] REM:  $n = 17, 15$  neurons; NREM:  $n = 16, 23$  neurons; [PFC] REM:  $n = 15, 17$  neurons; NREM:  $n = 15, 17$  neurons. Non-pyramidal neurons: [HPC] REM:  $n = 14, 13$  neurons; NREM:  $n = 11, 7$  neurons; [PFC] REM:  $n = 9, 11$  neurons; NREM:  $n = 10, 8$  neurons. **B:** Power spectra of signals in HPC and PFC during REM and NREM sleep. In the PFC, delta power was also enhanced ( $P = 0.028$ ). **C:** Co-modulation maps of cross-frequency coupling in the HPC during REM sleep and corresponding quantification of theta-high gamma MI. **D:** Quantification of relevant features of ripple events recorded during NREM sleep. A representative example of a ripple recorded in a mouse of the WT NE group is also shown.

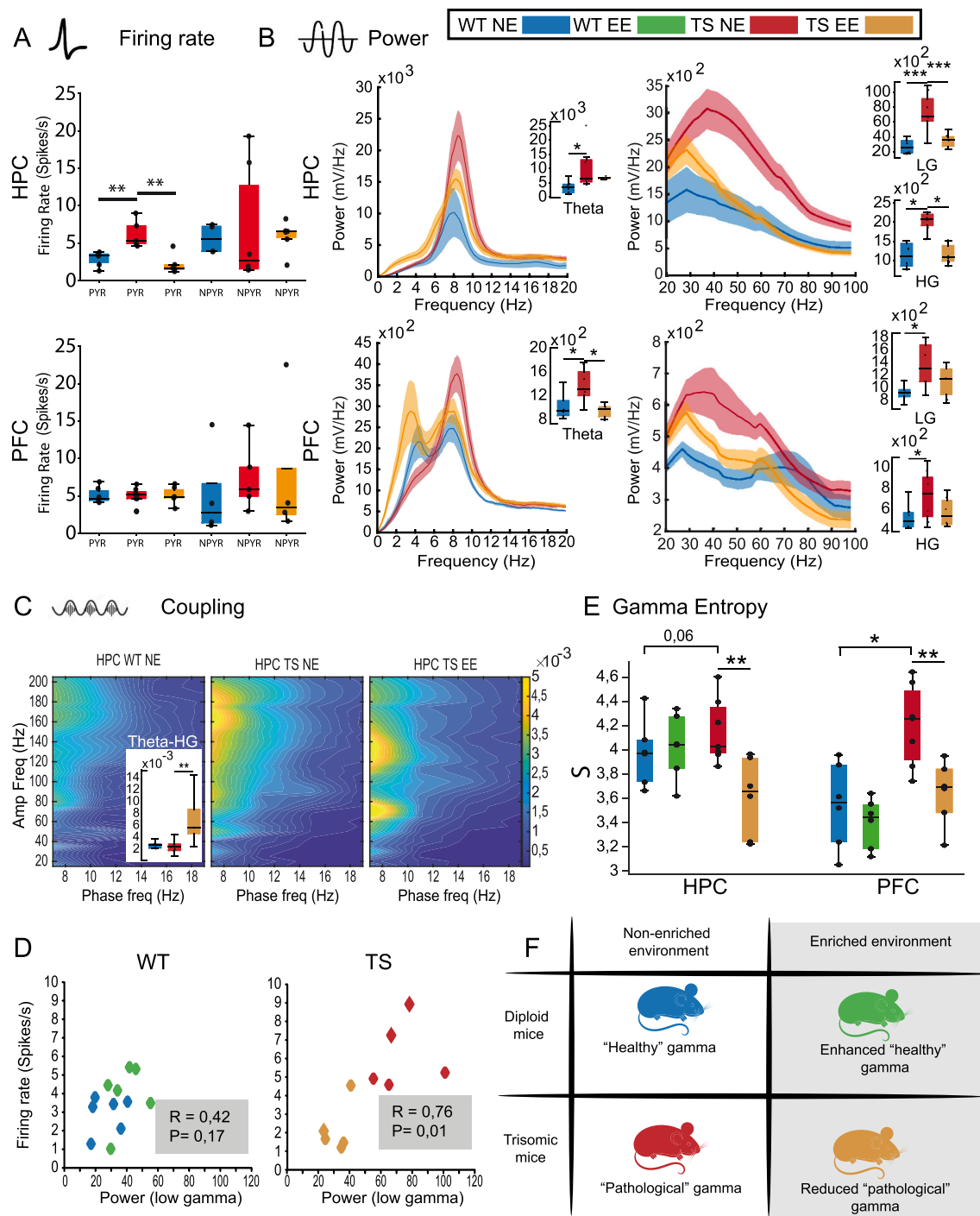
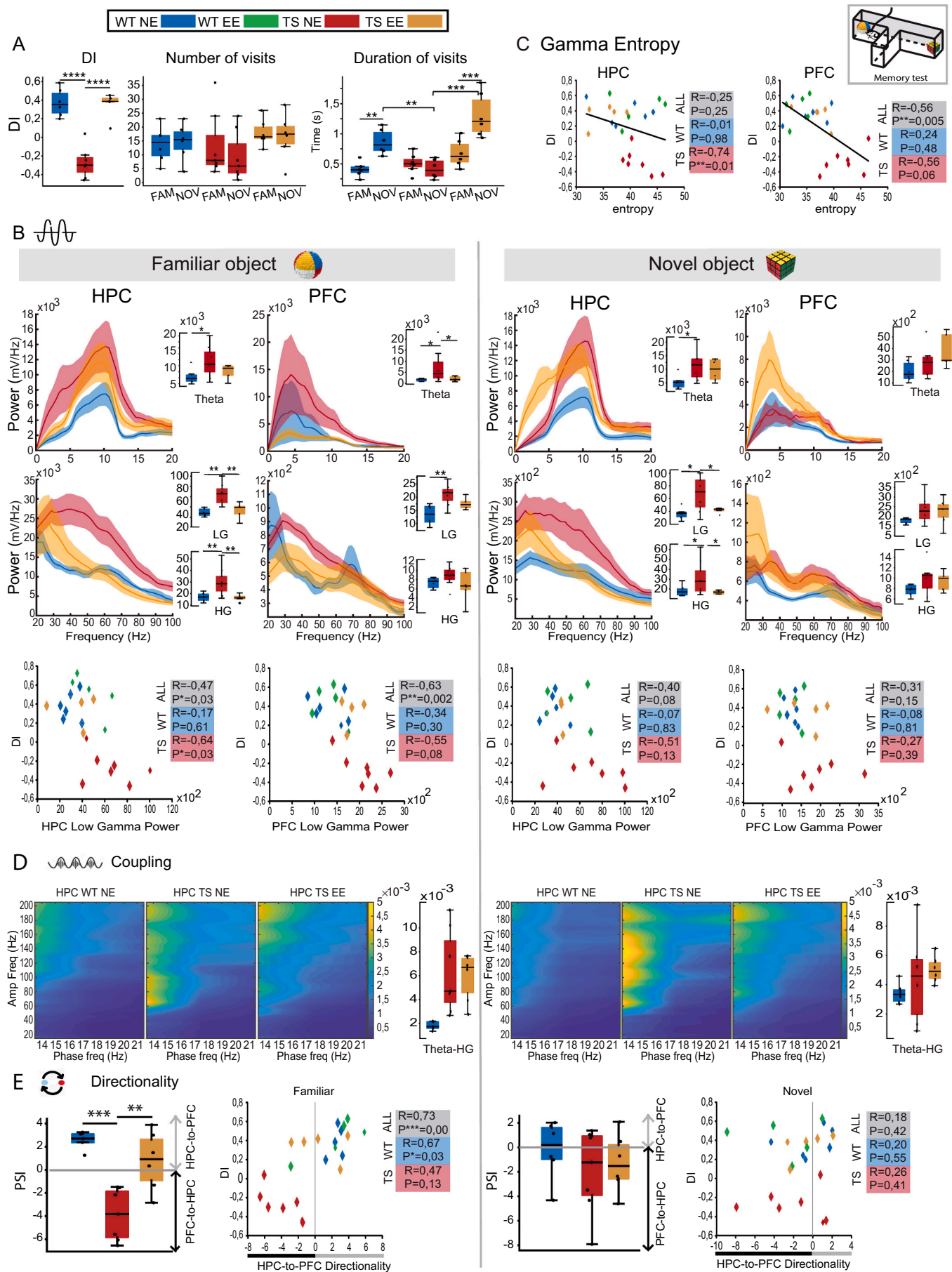


**Fig. 4.** EE prevents pathological theta and gamma hypersynchrony in Ts65Dn female mice during quiet wakefulness. **A:** Mean firing rates per animal in the HPC and PFC. Number of pyramidal neurons isolated in each brain region in trisomic NE and EE mice: [HPC]  $n = 26, 16$  neurons; [PFC]  $n = 28, 26$  neurons. Non-pyramidal neurons: [HPC]  $n = 12, 7$  neurons; [PFC]  $n = 8, 7$  neurons. **B:** Power spectra of signals in the HPC and PFC. Trisomic females exhibited enhanced theta and low/high gamma oscillations in the HPC (two-way ANOVA, genotype x rearing interaction;  $F_{1,21} = 8.614, 17.273, 11.34, P = 0.008, <0.0005, 0.003$ ; WT NE vs. TS NE mice,  $P = 0.011, <0.0005, 0.012$ ) and the PFC ( $F_{1,19} = 7.239, 4.436, P = 0.014, 0.048$ ; WT NE vs. TS NE mice,  $P = 0.043, 0.014, 0.046$ ) that were normalized in the TS EE group (TS EE vs. WT NE mice, [HPC theta, gamma]  $P = 0.15, 0.88$ ; [PFC theta, gamma]  $P = 0.51, 0.17$ ). **C:** Co-modulation maps of cross-frequency coupling in the HPC and corresponding quantification of theta-high gamma MI. **D:** Correlation between firing rate and gamma power recorded in the HPC. **E:** Quantification of low gamma entropy in the HPC and PFC for the four experimental groups. **F:** Proposed model for the effects of EE on gamma synchrony in diploid and trisomic mice reared in enriched and non-enriched environments. For visualization purposes, panels A to C omit the wild-type enriched group, which can be found in Fig. 1.

correlated with the DIs. This was consistent with our previous findings in male mice (Alemany-González et al., 2020). The strength of this gamma communication was similar between rearing groups, in accord with their comparable DIs (Mann-Whitney test,  $P = 0.42$ ; Fig. 2E). Conversely,

gamma signals recorded during the visits to novel objects did not show a clear directionality and were not associated with memory performances. We conclude that EE entrains hippocampal gamma oscillations and hippocampal-prefrontal gamma connectivity during memory retrieval.



(caption on next page)

**Fig. 5.** EE reduces theta and gamma hypersynchrony in Ts65Dn female mice during memory performance. A: Ts65Dn females exhibited poor memory performances that were fully rescued in TS enriched animals. This was due to an increase in the duration of visits to novel objects. B: Power spectra of signals during visits to familiar and novel objects are depicted on the left and right columns, respectively. Correlations between gamma power and DIs are shown below. During the visits to familiar objects, theta and low/high gamma power were increased in the HPC of trisomic females compared to their diploid peers (two-WAY ANOVA,  $F_{1,19} = 5.39$ ,  $13.41$ ,  $16.1$ ,  $P = 0.03$ ,  $0.002$ ,  $0.001$ ). During the visits to novel objects, theta and gamma power were also increased in the HPC of trisomic animals ( $F_{1,20} = 5.51$ ,  $5.56$ ,  $P = 0.03$ ; TS NE vs. WT NE:  $P = 0.01$ ,  $0.05$ ) whereas in the PFC it was less noticeable ( $F_{1,20} = 7.43$ ,  $5.44$ ,  $P = 0.013$ ,  $0.03$ ). In trisomic EE mice, the aberrant low/high gamma detected in the HPC was reduced to wild-type levels (TS NE vs. TS EE:  $P = 0.048$ ,  $0.038$ ; TS EE vs. WT NE:  $P = 0.36$ ,  $0.57$ ). C: Correlations between low gamma entropy during visits to familiar objects and DIs. D: Co-modulation maps of cross-frequency coupling in the HPC and corresponding quantification of theta-high gamma MIs. E: HPC-to-PFC directionality (PSI) at low gamma frequencies during visits to the objects. Corresponding correlations between gamma PSI and DIs are also shown. For visualization purposes, we omit the wild-type enriched group in the figure, which can be found in Fig. 2.

### 3.3. Environmental enrichment enhances hippocampal gamma synchrony and sharp wave ripples during sleep

We recorded neural activities during sleep following the familiarization phase, aiming to capture the processing of recently acquired memories (Fig. 2A). Rapid eye movement (REM) and non-rapid eye movement (NREM) episodes were detected during periods of low behavioral activity in an open field as previously reported (Alemany-González et al., 2020). In brief, REM sleep is characterized by prominent theta oscillations in the HPC whereas NREM sleep can be easily identified by the emergence of slow oscillations ( $<4$  Hz) in the cortex and sharp wave-ripple (SWR) events in the HPC (highly synchronous oscillatory activity at 100–250 Hz lasting  $\sim 100$ –200 ms) (Buzsáki, 2002; Steriade, 2006). Cortical slow waves and hippocampal ripples have been shown to contribute to offline information processing relevant for memory retrieval and consolidation (Buzsáki, 2015; Joo and Frank, 2018) and were therefore investigated here in detail.

During REM sleep, presumed pyramidal neurons in the HPC of EE mice tended to fire more action potentials than in NE mice but the difference did not reach significance ( $n = 6$  mice per group; mixed ANOVA, rearing x region interaction  $F_{1,20} = 0.5$ ,  $P = 0.68$ ; EE and NE: 2.44 and 1.61 spikes/s, respectively). No changes were detected for putative non-pyramidal neurons. During NREM sleep, the firing rates of pyramidal neurons were similar between rearing groups, however the spiking activity of non-pyramidal cells tended to decrease (Fig. 3A). Moreover, during REM sleep, as in quiet wake and memory performance, gamma oscillations were increased in the HPC of EE mice (mixed ANOVA,  $F_{1,8} = 5.959$ ,  $P = 0.04$ ; Fig. 3B) along with strengthening of theta-gamma coupling (8–10 with 40–80 cycles/s; Mann-Whitney test,  $P = 0.032$ ; Fig. 3C). Finally, ripple power was slightly larger in EE mice (unpaired *t*-test,  $P = 0.047$ ) while ripple number per minute, duration, frequency, and entropy were not different between groups (Fig. 3D).

### 3.4. Environmental enrichment reduces aberrant spiking and theta/gamma hypersynchrony in the HPC and PFC of Ts65Dn female mice during rest

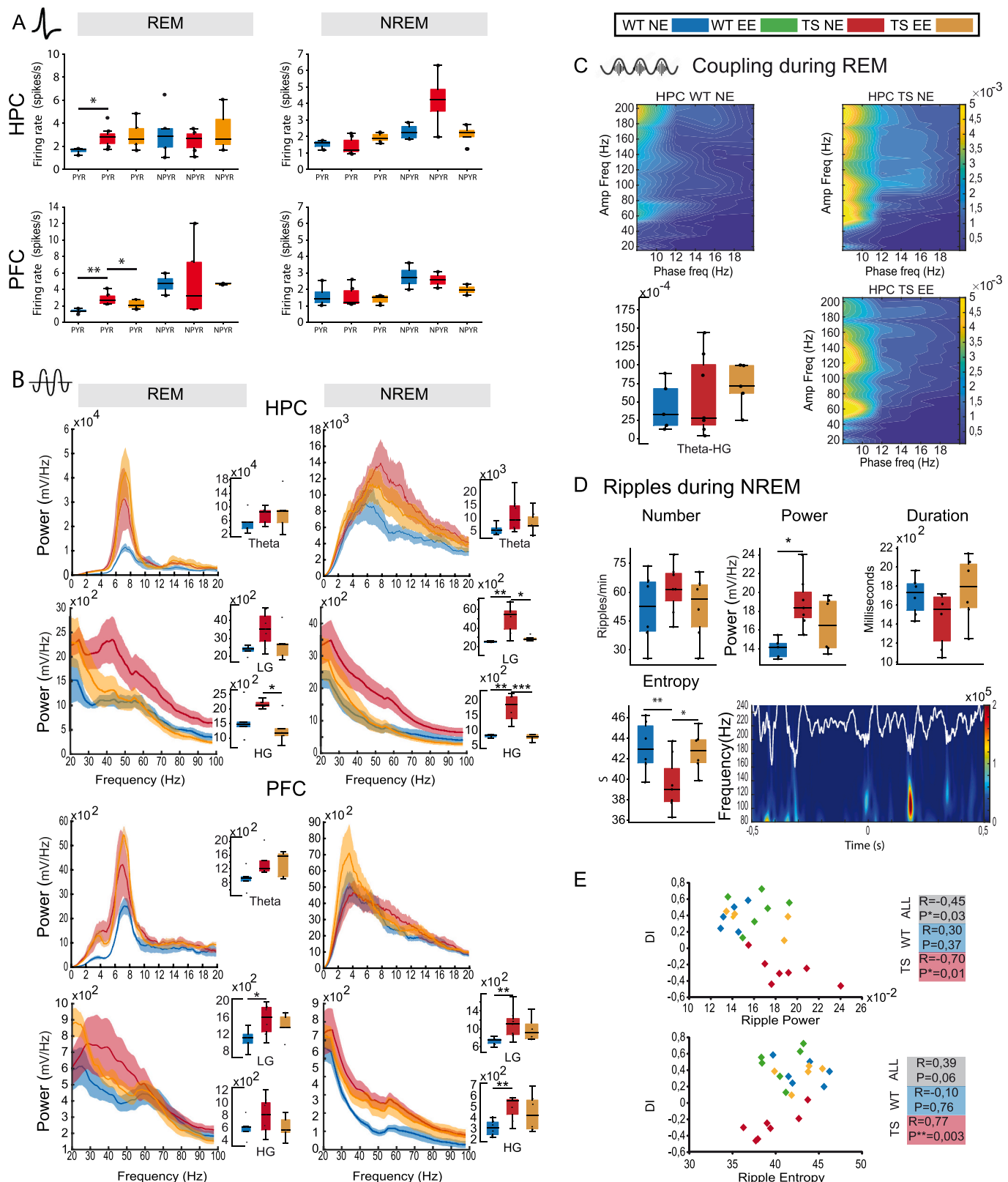
To further understand the pro-cognitive effects of postnatal EE we used the Ts65Dn trisomic mouse line, a well-established mouse model of DS. We investigated differential neural activities between wild-type (WT NE:  $n = 6$  mice) and trisomic mice and assessed the effects of rearing (TS NE, EE:  $n = 7$  and 6 mice, respectively). As in trisomic males (Alemany-González et al., 2020), presumed pyramidal neurons in the HPC of trisomic females displayed higher firing rates compared to their diploid counterparts during resting states (two-WAY ANOVA, genotype x region interaction:  $F_{1,17} = 15.28$ ,  $P < 0.001$ ; WT NE vs. TS NE,  $P = 0.007$ ). The trisomic EE group exhibited lower hippocampal spiking (TS EE ns vs. TS NE,  $P = 0.002$ ;  $n = 12$ , 22 neurons) with firing rates within the range of the wild types ( $P = 0.36$ ). In contrast, pyramidal activity in the PFC was similar between genotypes and seemed unaffected by rearing. Furthermore, inconsistent effects were observed in non-pyramidal neurons of both regions (Fig. 4A). Also consistent with trisomic males, trisomic females exhibited enhanced theta and low/high gamma oscillations in the HPC and the PFC (mixed ANOVA; Fig. 4B). Notably, low gamma

power in the HPC of TS NE mice almost doubled that observed in the WT EE group ( $P = 0.014$ ). We also note that excessive theta power in trisomic mice was not due to their inherent hyperlocomotion (Faizi et al., 2011) because the animals did not engage in activities associated with increased mobility while resting. Enhanced theta and gamma oscillations attenuated in the TS EE group and oscillatory power was close to that observed in diploid animals (Fig. 4B). Trisomic females also exhibited broad cross-frequency coupling between theta waves and oscillations at high frequencies ( $>80$  Hz) in the HPC compared to their non-trisomic peers. In the TS EE group, coupling between theta and high gamma was selectively enhanced in similar patterns than those observed in WT EE mice (Kruskal-Wallis test, rearing factor  $P < 0.001$ ; TS EE vs. TS NE,  $P = 0.026$ ; Fig. 4C), suggesting an improved signal-to-noise ratio of hippocampal activity in TS EE animals.

Taken together, our results indicated opposite effects of EE on gamma rhythms in diploid and trisomic animals. That is, enhancement of hippocampal gamma in enriched wild-types and reduction of aberrant gamma in the HPC and PFC of trisomic mice. Based on recent literature (Guyon et al., 2021), we hypothesized that EE favored “healthy” gamma rhythms in diploid animals, gamma synchrony emerging from the interplay between fast-spiking interneurons and pyramidal neurons, and reduced “pathological” gamma rhythms in trisomic animals, gamma synchrony generated by the increase of asynchronous or “noisy” firing of pyramidal neurons due to inhibitory dysfunction. The increased pyramidal firing in the HPC correlated with low gamma power in trisomic but not in wild-type mice (Fig. 4D), in accordance with a LFP “contamination” by asynchronous neuronal firing (Guyon et al., 2021). We next estimated the entropy of the LFP signals, as increased entropy has been linked to pathological synchronization in epilepsy and schizophrenia (Guyon et al., 2021; Valero et al., 2017). Trisomic mice exhibited increased low gamma entropy in the HPC and the PFC (Kruskal-Wallis test, genotype and rearing as factors; TS NE vs. WT NE:  $P = 0.057$ ,  $0.014$ ) that was reduced in the enriched group (TS NE vs. TS EE:  $P = 0.008$  in both regions). EE did not produce major effects on gamma entropy in diploid mice (Fig. 4E). Altogether, these results suggested that postnatal EE enhanced “healthy” gamma rhythms in wild-type mice and prevented the emergence of “pathological” gamma rhythms in trisomic animals (Fig. 4F).

### 3.5. Environmental enrichment reduces aberrant theta-gamma hypersynchrony in the HPC and PFC of Ts65Dn female mice during memory performance

Trisomic females performed poorly in the memory test ( $n = 7$  mice, mean DI  $-0.27 \pm 0.06$ ; two-WAY ANOVA, genotype x rearing interaction,  $F_{1,20} = 13.196$ ,  $P = 0.002$ ; TS NE vs. WT NE,  $P < 0.001$ ) while trisomic EE females performed like the wild types ( $n = 6$  mice, mean DI  $0.35 \pm 0.07$ ; TS NE vs. TS EE,  $P < 0.001$ ; TS NE vs. WT NE,  $P > 0.05$ ; Fig. 5A). The negative memory indices in trisomic NE mice resulted from the fact that the visits to novel items were shorter than those of diploid mice (509 ms in TS NE mice vs. 840 ms in WT NE mice;  $F_{1,19} = 4.469$ ,  $P = 0.04$ ; post hoc comparison  $P = 0.03$ ). Trisomic EE mice, like the wild types, visited novel objects longer than familiar objects (1310 ms vs. 677 ms, respectively; paired *t*-test,  $P = 0.0005$ ; TS EE mice vs. TS NE mice,  $P = 0.04$ ; Fig. 5A).



(caption on next page)

**Fig. 6.** Environmental enrichment rescues enhanced hippocampal-prefrontal gamma synchrony and ripple activity in Ts65Dn mice during sleep. A: Mean firing rates per animal in the HPC and PFC during REM and NREM sleep. Number of presumed pyramidal neurons isolated in each brain region and brain state in trisomic NE and EE mice: [HPC] REM:  $n = 24, 15$  neurons; NREM:  $n = 28, 16$  neurons; [PFC] REM:  $n = 31, 19$  neurons; NREM:  $n = 25, 20$  neurons. Non-pyramidal neurons: [HPC] REM:  $n = 19, 9$  neurons; NREM:  $n = 9, 13$  neurons; [PFC] REM:  $n = 11, 11$  neurons; NREM:  $n = 10, 7$  neurons. B: Power spectra of signals in the HPC and PFC with quantification of relevant bands. During REM sleep, trisomic NE mice showed augmented gamma oscillations in both brain regions (HG HPC, LG PFC:  $F_{1,18} = 8.76, 5.86, P = 0.008, 0.026$ ) that was decreased in trisomic EE animals. During NREM sleep, low and high gamma rhythms in the HPC and PFC were augmented in trisomic NE animals ( $F_{1,16} = 8.07, 17.52, 11.73, 13.45, P = 0.012, 0.001, 0.008, 0.001$ ) and were reduced in the HPC of the trisomic EE group. C: Co-modulation maps of cross-frequency coupling in the HPC during REM sleep and corresponding quantification of theta-high gamma MI. D: Quantification of relevant features of ripple events recorded during NREM sleep. Lower-right panel: representative example of a ripple recorded in a mouse of the TS NE group (same scale as the color plot shown in Fig. 3D). E: Correlations between ripple power and ripple entropy with discrimination indices (DIs) in the four groups. For visualization purposes, we omit the wild-type enriched group in the figure. The results for this group can be found in Fig. 3.

We next investigated neurophysiological divergences in Ts65Dn mice during memory retrieval and acquisition. During the visits to familiar objects, theta and low/high gamma power were increased in the HPC of trisomic females compared to their diploid peers (two-WAY ANOVA, Fig. 5B), similar to quiet wakefulness. Also as above, theta power increases were not simply due to hyperlocomotion of trisomic mice, as the animals' mobility was low while they were visiting the objects. Aberrant theta/gamma power lessened in the TS EE group, particularly gamma oscillations. In the PFC, trisomic mice showed less pronounced increases of theta and low gamma power that were also reduced in the EE group. Notably, low gamma power in the HPC of trisomic animals, but not of diploid animals, correlated inversely with DIs, while in the PFC these associations were weaker (Fig. 5B). Thus, these results put forward the pathological nature of gamma rhythms in trisomic animals, particularly in the HPC, and their strong negative impact on memory. This was further supported by significant correlations between gamma entropy in the HPC of TS NE animals and their poor memory performances ( $R = -0.74, P = 0.006$ ; Fig. 5C). We note that these correlations were significant for the TS group alone, therefore they did not simply emerge from the WT vs TS divergences per se. Power changes during the visits to novel objects were comparable to those detected during the visits to familiar objects. That is, theta and gamma power were increased in the HPC of trisomic animals whereas in the PFC they were less noticeable. In trisomic EE mice, the aberrant low/high gamma detected in the HPC was reduced to wild-type levels while no major effects of enrichment were observed in the PFC at these bands (two-WAY ANOVA, Fig. 5B). Moreover, we did not find significant associations between low gamma power and memory indices in either brain region (Fig. 5B).

Furthermore, like in resting states, trisomic NE mice exhibited broad hippocampal coupling between theta and high frequencies ( $>60$  Hz) both during the visits to familiar and novel items. However, the theta-high gamma coupling observed in diploid EE animals was not promoted in the trisomic EE group (Fig. 5D). Also, during the visits to familiar objects the selective HPC→PFC low gamma signals observed in diploid animals reversed in trisomic mice, originating in the PFC and traveling to the HPC (Kruskal-Wallis test, genotype and rearing as factors; genotype factor  $P < 0.008$ ; TS NE vs. WT NE,  $P = 0.003$ ). The circuit's information flow was rescued in several trisomic EE mice but was not fully restored in all the animals (TS EE vs. WT NE,  $P = 0.33$ ; Fig. 5E). As we previously reported for male mice, HPC→PFC low gamma signals correlated strongly with memory indices in the diploid group but not in the trisomic group, implicating HPC→PFC gamma communication in the neural correlates of recognition memory in both genders. This was further supported by multiple regression analyses. A combination of HPC→PFC low gamma signals and low gamma power in the HPC and PFC during the visits to familiar objects in all animals could predict DIs ( $F_{3,17} = 8.546, P = 0.001, R^2 = 0.58$ ), HPC→PFC gamma signals being the main contributors to the prediction ( $P = 0.013$ ). During the visits to novel objects, as in the wild types, we did not detect a clear directionality of signals and therefore there were no differences between genotypes or rearing conditions and no associations with memory indices (Fig. 5E).

### 3.6. Environmental enrichment attenuates aberrant hippocampal-prefrontal gamma synchrony and ripple activity in Ts65Dn mice during sleep

During REM sleep trisomic NE mice ( $n = 7$ ) manifested many of the neural activity alterations observed during quiet wake and memory performance. However, these were only partially rescued in trisomic enriched animals ( $n = 6$ ). First, many presumed pyramidal neurons in the HPC and PFC of TS NE mice exhibited elevated firing rates (two-way ANOVA, genotype x rearing interaction,  $F_{1,17} = 5.2, 9.69, P = 0.036, 0.006$ ), and this was only partially prevented in the PFC by EE ( $P = 0.11$ ; Fig. 6A). Second, trisomic mice also showed augmented theta and gamma oscillations in both brain regions. Abnormal gamma oscillations were reduced in the HPC and the PFC of enriched animals while excessive theta oscillations remained enhanced (two-way ANOVA; Fig. 6B). Cross-frequency coupling was indeed improved in EE trisomic animals where theta-high gamma coordination was better defined, suggesting an improved signal-to-noise ratio within hippocampal microcircuits (Kruskal-Wallis, genotype and rearing as factors;  $P < 0.05$ ; Fig. 6C).

During NREM sleep trisomic NE mice exhibited similar firing rates of putative pyramidal neurons in the HPC similar to their trisomic EE peers and the wild types (Fig. 6A). Firing rates of neurons in the PFC were also unaffected by genotype or rearing. Moreover, as in all the other brain states, low and high gamma rhythms in the HPC and PFC were augmented in trisomic NE animals, and they were reduced in enriched mice only in the HPC (Fig. 6B). In addition, in the PFC, slow waves were not different between any of the groups. Furthermore, ripple events exhibited increased power (2-way ANOVA, genotype x rearing interaction;  $F_{1,20} = 5.56, P = 0.029$ ) and reduced entropy (Kruskal-Wallis test;  $P < 0.05$ ) in trisomic mice that were normalized in many EE animals (TS EE vs. WT NE,  $P = 0.1, 0.7$ ; Fig. 6D). We note that entropy during ripples in TS mice was reduced and not increased as in other brain states. Ripple power and entropy recorded in the trisomic group correlated inversely with memory indices thus predicting poor memory performances (Fig. 6E).

Finally, we performed multiple regression analyses to provide further support to the significance of the correlations observed in the study. We identified three biomarkers recorded in three different brain states that seemed relevant to explain memory performances and correlated with memory indices: low gamma power in the HPC during resting, HPC→PFC gamma signals during the visits to familiar objects, and ripple power during NREM sleep. Multiple regression models could predict the DIs when combining the three biomarkers in all the mice ( $F_{3,17} = 8.36, P = 0.001, R^2 = 0.593$ ), HPC→PFC gamma signals and ripple power being main contributors to the prediction ( $P = 0.015$  and  $0.023$ , respectively) whereas HPC gamma power only had marginal contribution ( $P = 0.819$ ). This is in line with our previous observations in males, where circuit connectivity and ripple amplitude seemed critical for memory performance (Alemany-González et al., 2020).

#### 4. Discussion

We report that physical, social, and cognitive stimulation during critical developmental periods shapes hippocampal neural dynamics in wild-type mice and prevents the disruption of hippocampal-prefrontal pathways in a mouse model of intellectual disability. Diploid animals reared in enriched environments exhibited enhanced pyramidal spiking, gamma rhythms and sleep ripples in the HPC. Conversely, in trisomic mice theta and gamma power were increased in the HPC and PFC across distinct brain states, sleep ripples were abnormal, and circuit gamma communication was disrupted during memory retrieval. These alterations were attenuated in their environmentally enriched peers.

Wild-type mice reared in stimulating environments exhibited enhanced pyramidal activity and gamma synchrony within hippocampal microcircuits across different brain states. We note that non-pyramidal neurons likely included a variety of interneuron subtypes for which it was difficult to obtain consistent effects. Concomitantly, hippocampal gamma synchrony (power and coupling with theta waves) was consistently enhanced during resting, memory performance, and REM sleep. These findings are in line with previous observations reporting increased gamma oscillations in the HPC of anesthetized rodents reared in enriched environments (Shinohara et al., 2013; Tanaka et al., 2017) and provide new evidence for experience-dependent enhancement of hippocampal gamma synchrony during alertness, sleep and memory performance. Furthermore, our observations of enhanced sleep ripples in the EE group were also reported previously in anesthetized mice (Tanaka et al., 2017). Here, ripples were recorded during episodes of NREM sleep immediately after the familiarization phase, thus their enhancement may reflect more efficacious memory acquisition and consolidation in enriched animals (Buzsáki, 2015; Joo and Frank, 2018). Moreover, our findings unraveled again strong associations between HPC→PFC low gamma signals recorded during the visits to familiar objects and discrimination indices, confirming that both male and female mice with robust HPC→PFC gamma connectivity exhibit superior memory performances in the NOR task (Alemany-González et al., 2020). Conflicting results exist on whether recognition memory for objects requires the PFC (Spanswick and Dyck, 2012; Morici et al., 2015). A recent study however implicates the medial PFC in this type of memory via optogenetic interrogation and identifies HPC→PFC coupling as a major neural mechanism involved (Wang et al., 2021). In summary, the neurophysiological changes identified here in enriched wild-type animals combined task-independent adjustments (augmented hippocampal pyramidal activity and gamma synchrony across different brain states) and memory-dependent adjustments (enhanced theta-gamma coupling and ripples in the HPC associated with memory retrieval).

Non-enriched trisomic females exhibited robust increases in theta and gamma power in the HPC and PFC across all brain states. This is in line with previous studies reporting increased theta-gamma oscillations and synchrony within hippocampal-prefrontal pathways in mouse models of DS and other intellectual disabilities (Arbab et al., 2018; Chang et al., 2020; Ramon-Duaso et al., 2019). Here, we also detected broad theta-high frequency coupling and enlarged ripples in the HPC. Finally, trisomic mice exhibited reversed HPC→PFC gamma connectivity during memory retrieval. Aberrant theta, gamma, ripple power and circuit miscommunication were also observed in trisomic male mice of the same transgenic line (Alemany-González et al., 2020), demonstrating similar aberrant synchrony in DS subjects of both genders. In fact, they predicted poor memory performances and were attenuated in trisomic EE animals, unraveling their critical involvement in memory processing. These results suggest that normalizing hippocampal-prefrontal hypersynchrony and miscommunication are major neural mechanisms underlying the beneficial effects of EE in intellectual disability.

EE enhanced gamma synchrony in diploid mice and reduced aberrant gamma synchrony in trisomic mice. How can this be reconciled?

One possibility is that the hypersynchrony observed in DS animals was well above the levels of those observed in enriched diploid animals. We found that this was the case for hippocampal gamma, but not for pre-frontal gamma. This implies an inverted-U shaped range of gamma synchrony in the HPC for optimal memory performance, whereby insufficient or excessive gamma is detrimental to memory. Another plausible explanation is that distinct neural mechanisms underlie “healthy” and “pathological” gamma synchronization. A widely accepted hypothesis is that elevation in the ratio of cellular excitation to inhibition could give rise to increased gamma oscillations that would result in social and cognitive deficits like the ones observed in patients with autism and schizophrenia (Sohal and Rubenstein, 2019; Yizhar et al., 2011). In fact, enhanced broadband gamma can arise from asynchronous activities that result from deficient inhibition and increased, but desynchronized, pyramidal activity (Guyon et al., 2021). “Healthy” gamma would arise from a true synchronization of neural activity whereas “pathological” gamma would arise from asynchronous hyperactivity. In support of this, in this study pyramidal spiking and LFP entropy, a measure of asynchrony, in the HPC and PFC were increased in trisomic mice and predicted pathological gamma power. Likewise, ripple power was augmented in diploid enriched mice but was even larger in trisomic animals. Ripples arise from the excitatory recurrent CA3→CA1 system and their activity is coordinated by a consortium of interneurons (Buzsáki, 2015). Pathological ripples may emerge from unbalanced inhibition of neural networks that cause broad disruptions of sleep patterns in individuals with DS and in DS mouse models (Raveau et al., 2018; Ruiz-Mejias, 2019). Together, these findings provide new insight into the GABAergic dysfunction observed in DS. Although our study failed to detect consistent alterations in the neural activities of GABAergic interneurons in trisomic animals, our findings challenge the widely accepted hypothesis of overinhibition of principal cells in DS. They indeed suggest deficient inhibition of hippocampal-prefrontal neural networks *in vivo* in DS that result in increased and disorganized spiking activity of principal neurons. These results are in line with recent investigations that propose that a disturbed inhibitory tone rather than a generalized overinhibition underlies some of the characteristic cognitive deficits in DS (Valbuena et al., 2021).

In a previous study conducted in Ts65Dn males we investigated the neural substrates underlying the rescuing abilities of a green tea extract containing epigallocatechin-3-gallate (EGCG) (Alemany-González et al., 2020), a DYRK1A kinase inhibitor with pro-cognitive effects in individuals with DS (de la Torre et al., 2016). Considering that equivalent pathological synchrony was detected in Ts65Dn females and males, this study provides unique insights into the comparative rescuing effects of EE and EGCG in the same mouse model of DS. We found that both pro-cognitive treatments attenuated aberrant theta, gamma, and ripple power within the circuit and corrected HPC→PFC gamma directionality during memory retrieval. Green tea extracts, EE and their combination restored >70% of the phosphoprotein deregulation in Ts65Dn mice while re-establishment of a proper epigenetic state and rescue of the kinome deregulation may contribute to the cognitive rescue induced by green tea extracts (De Toma et al., 2020). Future studies should investigate the neural substrates of a combination of EE and EGCG in diploid and trisomic animals. We also note that the Ts65Dn model is known to contain additional genes not triplicated in human DS (Constestabile et al., 2017) that might impact the phenotypes observed here. Therefore, it would be important to confirm the findings presented here in other mouse lines of DS.

#### 5. Concluding remarks

In closing, neural activities associated with brain state adjustments and memory-associated adjustments in the HPC are good candidates to underlie the beneficial effects of EE on cognition in wild-type mice. Concomitantly, EE attenuates hippocampal and prefrontal pathological hypersynchrony in trisomic mice. This strongly suggests distinct neural

mechanisms for the generation and rescue of healthy and pathological brain synchrony, respectively, by EE.

### CRediT authorship contribution statement

**Maria Alemany-González:** Conceptualization, Investigation, Formal analysis, Visualization, Writing – original draft, Writing – review & editing. **Marta Vilademunt:** Formal analysis, Visualization, Writing – review & editing. **Thomas Gener:** Conceptualization, Investigation, Visualization, Supervision, Writing – review & editing. **M. Victoria Puig:** Conceptualization, Supervision, Formal analysis, Writing – original draft, Writing – review & editing, Funding acquisition.

### Declaration of Competing Interest

None.

### Data availability

Data will be made available on request.

### Acknowledgements

We are grateful to Mara Dierssen and Jose A. Garrido for providing scientific insight and to Manuel Valero for providing scripts to analyze ripple activity and entropy. We also thank Pau Nebot for excellent technical support. This work was supported by the Jerome Lejeune Foundation (grant #1419) and by the Spanish government grants SAF2016-80726-R and PID2019-104683RB-I00 funded by MCIN/AEI/10.13039/501100011033 and by ERDF “A way of making Europe”.

### References

Alemany-González, M., Gener, T., Nebot, P., Vilademunt, M., Dierssen, M., Puig, M.V., 2020. Prefrontal-hippocampal functional connectivity encodes recognition memory and is impaired in intellectual disability. *Proc. Natl. Acad. Sci.* 117, 11788–11798. <https://doi.org/10.1073/pnas.1921314117>.

Anagnostopoulou, A., Styliadis, C., Kartsidis, P., Romanopoulou, E., Zilidou, V., Karali, C., Karagianni, M., Klados, M., Paraskevopoulos, E., Bamidis, P.D., 2021. Computerized physical and cognitive training improves the functional architecture of the brain in adults with Down syndrome: a network science EEG study. *Netw. Neurosci. Camb. Mass.* 5, 274–294. [https://doi.org/10.1162/netn\\_a\\_00177](https://doi.org/10.1162/netn_a_00177).

Anderson, J.S., Nielsen, J.A., Ferguson, M.A., Burback, M.C., Cox, E.T., Dai, L., Gerig, G., Edgin, J.O., Korenberg, J.R., 2013. Abnormal brain synchrony in Down syndrome. *NeuroImage Clin.* 2, 703–715. <https://doi.org/10.1016/j.nic.2013.05.006>.

Arbab, T., Battaglia, F.P., Pennartz, C.M.A., Bosman, C.A., 2018. Abnormal hippocampal theta and gamma hypersynchrony produces network and spike timing disturbances in the Fmr1-KO mouse model of Fragile X syndrome. *Neurobiol. Dis.* 114, 65–73. <https://doi.org/10.1016/j.nbd.2018.02.011>.

Begenisic, T., Spolidoro, M., Braschi, C., Baroncelli, L., Milanese, M., Pietra, G., Fabbri, M.E., Bonanno, G., Cioni, G., Maffei, L., Sale, A., 2011. Environmental enrichment decreases GABAergic inhibition and improves cognitive abilities, synaptic plasticity, and visual functions in a mouse model of Down syndrome. *Front. Cell. Neurosci.* 5, 29. <https://doi.org/10.3389/fncel.2011.00029>.

Begenisic, T., Sansevero, G., Baroncelli, L., Cioni, G., Sale, A., 2015. Early environmental therapy rescues brain development in a mouse model of Down syndrome. *Neurobiol. Dis.* 82, 409–419. <https://doi.org/10.1016/j.nbd.2015.07.014>.

Belenković, P.V., Kleschevnikov, A.M., Salehi, A., Epstein, C.J., Mobley, W.C., 2007. Synaptic and cognitive abnormalities in mouse models of Down syndrome: exploring genotype-phenotype relationships. *J. Comp. Neurol.* 504, 329–345. <https://doi.org/10.1002/cne.21433>.

Bokil, H., Andrews, P., Kulkarni, J.E., Mehta, S., Mitra, P.P., 2010. Chronux: a platform for analyzing neural signals. *J. Neurosci. Methods* 192, 146–151. <https://doi.org/10.1016/j.jneumeth.2010.06.020>.

Brenes, J.C., Lackinger, M., Högländer, G.U., Schrott, G., Schwarting, R.K.W., Wöhr, M., 2016. Differential effects of social and physical environmental enrichment on brain plasticity, cognition, and ultrasonic communication in rats. *J. Comp. Neurol.* 524, 1586–1607. <https://doi.org/10.1002/cne.23842>.

Buzsáki, G., 2002. Theta oscillations in the hippocampus. *Neuron* 33, 325–340.

Buzsáki, G., 2015. Hippocampal sharp wave-ripple: a cognitive biomarker for episodic memory and planning. *Hippocampus* 25, 1073–1188. <https://doi.org/10.1002/hipo.22488>.

Chang, P., Bush, D., Schorge, S., Good, M., Canonica, T., Shing, N., Noy, S., Wiseman, F. K., Burgess, N., Tybulewicz, V.L.J., Walker, M.C., Fisher, E.M.C., 2020. Altered hippocampal-prefrontal neural dynamics in mouse models of Down syndrome. *Cell Rep.* 30, 1152–1163 e4. <https://doi.org/10.1016/j.celrep.2019.12.065>.

Conestabile, A., Magara, S., Cancedda, L., 2017. The GABAergic hypothesis for cognitive disabilities in Down syndrome. *Front. Cell. Neurosci.* 11, 54. <https://doi.org/10.3389/fncel.2017.00054>.

Cramer, N., Galdzicki, Z., 2012. From abnormal hippocampal synaptic plasticity in down syndrome mouse models to cognitive disability in Down syndrome. *Neural Plast.* 2012, 101542. <https://doi.org/10.1155/2012/101542>.

De la Torre, R., de Sola, S., Hernández, G., Farré, M., Puig, J., Rodríguez, J., Espadaler, J. M., Langohr, K., Cuenca-Royo, A., Príncipe, A., Xicoté, L., Jane, N., Catuara-Solarz, S., Sanchez-Benavides, G., Bléhaut, H., Dueñas-Espín, I., del Hoyo, L., Benejam, B., Blanco-Hinojo, L., Videla, S., Fitó, M., Delabar, J.M., Dierssen, M., TESDAD study group, 2016. Safety and efficacy of cognitive training plus epigallocatechin-3-gallate in young adults with Down's syndrome (TESDAD): a double-blind, randomised, placebo-controlled, phase 2 trial. *Lancet Neurol.* 15, 801–810. [https://doi.org/10.1016/S1474-4422\(16\)30034-5](https://doi.org/10.1016/S1474-4422(16)30034-5).

De Toma, I., Ortega, M., Aloy, P., Sabidó, E., Dierssen, M., 2019. DYRK1A overexpression alters cognition and neural-related proteomic pathways in the hippocampus that are rescued by green tea extract and/or environmental enrichment. *Front. Mol. Neurosci.* 12 <https://doi.org/10.3389/fnmol.2019.00272>.

De Toma, I., Ortega, M., Catuara-Solarz, S., Sierra, C., Sabidó, E., Dierssen, M., 2020. Re-establishment of the epigenetic state and rescue of kinase deregulation in Ts65Dn mice upon treatment with green tea extract and environmental enrichment. *Sci. Rep.* 10, 16023. <https://doi.org/10.1038/s41598-020-72625-z>.

Delgado-Sallent, C., Nebot, P., Gener, T., Fath, A.B., Timplalexi, M., Puig, M.V., 2021. Atypical, but not typical, antipsychotic drugs reduce hypersynchronized prefrontal-hippocampal circuits during psychosis-like states in mice: contribution of 5-HT2A and 5-HT1A receptors. *Cereb. Cortex N Y N* 1991 bhab427. <https://doi.org/10.1093/cercor/bhab427>.

Faiz, M., Bader, P.L., Tun, C., Encarnacion, A., Kleschevnikov, A., Belichenko, P., Saw, N., Priestley, M., Tsien, R.W., Mobley, W.C., Shamloo, M., 2011. Comprehensive behavioral phenotyping of Ts65Dn mouse model of Down syndrome: activation of  $\beta$ 1-adrenergic receptor by xamoterol as a potential cognitive enhancer. *Neurobiol. Dis.* 43, 397–413. <https://doi.org/10.1016/j.nbd.2011.04.011>.

Figueroa-Jimenez, M.D., Cañete-Massé, C., Carbó-Carreté, M., Zarabozo-Hurtado, D., Peró-Cebollero, M., Salazar-Estrada, J.G., Guàrdia-Olmos, J., 2021. Resting-state default mode network connectivity in young individuals with Down syndrome. *Brain Behav.* 11, e01905 <https://doi.org/10.1002/brb3.1905>.

Gener, T., Tauste-Campo, A., Alemany-González, M., Nebot, P., Delgado-Sallent, C., Chanovas, J., Puig, M.V., 2019. Serotonin 5-HT1A, 5-HT2A and dopamine D2 receptors strongly influence prefrontal-hippocampal neural networks in alert mice: contribution to the actions of risperidone. *Neuropharmacology* 158, 107743. <https://doi.org/10.1016/j.neuropharm.2019.107743>.

Gulinello, M., Mitchell, H.A., Chang, Q., Timothy O'Brien, W., Zhou, Z., Abel, T., Wang, L., Corbin, J.G., Veeraraghavan, S., Samaco, R.C., Andrews, N.A., Fagiolini, M., Cole, T.B., Burbacher, T.M., Crawley, J.N., 2018. Rigor and reproducibility in rodent behavioral research. *Neurobiol. Learn. Mem.* S1074-7427, 30001–30007. <https://doi.org/10.1016/j.jnl.2018.01.001>.

Guyon, N., Zacharias, L.R., de Oliveira, E.F., Kim, H., Leite, J.P., Lopes-Aguiar, C., Carlén, M., 2021. Network asynchrony underlying increased broadband gamma power. *J. Neurosci.* <https://doi.org/10.1523/JNEUROSCI.2250-20.2021>.

Hirase, H., Shinohara, Y., 2014. Transformation of cortical and hippocampal neural circuit by environmental enrichment. *Neuroscience* 280, 282–298. <https://doi.org/10.1016/J.NEUROSCIENCE.2014.09.031>.

Jensen, O., Colgin, L.L., 2007. Cross-frequency coupling between neuronal oscillations. *Trends Cogn. Sci.* 11, 267–269. <https://doi.org/10.1016/j.tics.2007.05.003>.

Joo, H.R., Frank, L.M., 2018. The hippocampal sharp wave-ripple in memory retrieval for immediate use and consolidation. *Nat. Rev. Neurosci.* 19, 744–757. <https://doi.org/10.1038/s41583-018-0077-1>.

Karaaslan, O., Mahoney, G., 2013. Effectiveness of responsive teaching with children with Down syndrome. *Intellect. Dev. Disabil.* 51, 458–469. <https://doi.org/10.1352/1934-9556-51.6.458>.

Kim, H., Ahrlund-Richter, S., Wang, X., Deisseroth, K., Carlén, M., 2016. Prefrontal parvalbumin neurons in control of attention. *Cell* 164, 208–218. <https://doi.org/10.1016/j.cell.2015.11.038>.

Kleschevnikov, A.M., Belichenko, P.V., Villar, A.J., Epstein, C.J., Malenka, R.C., Mobley, W.C., 2004. Hippocampal long-term potentiation suppressed by increased inhibition in the Ts65Dn mouse, a genetic model of Down syndrome. *J. Neurosci.* 24, 8153–8160. <https://doi.org/10.1523/JNEUROSCI.1766-04.2004>.

Leger, M., Quièdeville, A., Bouet, V., Haelewyn, B., Boulouard, M., Schumann-Bard, P., Freret, T., 2013. Object recognition test in mice. *Nat. Protoc.* 8, 2531–2537. <https://doi.org/10.1038/nprot.2013.155>.

Leger, M., Paizanis, E., Dzahini, K., Quièdeville, A., Bouet, V., Cassel, J.-C., Freret, T., Schumann-Bard, P., Boulouard, M., 2015. Environmental enrichment duration differentially affects behavior and neuroplasticity in adult mice. *Cereb. Cortex* 25, 4048–4061. <https://doi.org/10.1093/cercor/bhu119>.

Livingston, G., Sommerlad, A., Ortega, V., Costafreda, S.G., Huntley, J., Ames, D., Ballard, C., Banerjee, S., Burns, A., Cohen-Mansfield, J., Cooper, C., Fox, N., Giltn, L. N., Howard, R., Kales, H.C., Larson, E.B., Ritchie, K., Rockwood, K., Sampson, E.L., Samus, Q., Schneider, L.S., Selbæk, G., Teri, L., Mukadam, N., 2017. Dementia prevention, intervention, and care. *Lancet Lond. Engl.* 390, 2673–2734. [https://doi.org/10.1016/S0140-6736\(17\)31363-6](https://doi.org/10.1016/S0140-6736(17)31363-6).

Martínez Cué, C., Dierssen, M., 2020. Plasticity as a therapeutic target for improving cognition and behavior in Down syndrome. In: *Progress in Brain Research*. Elsevier B.V, pp. 269–302. <https://doi.org/10.1016/bs.pbr.2019.11.001>.

Martínez-Cué, C., Baamonde, C., Lumbreiras, M., Paz, J., Davisson, M.T., Schmidt, C., Dierssen, M., Flórez, J., 2002. Differential effects of environmental enrichment on behavior and learning of male and female Ts65Dn mice, a model for Down

syndrome. *Behav. Brain Res.* 134, 185–200. [https://doi.org/10.1016/s0166-4328\(02\)00026-8](https://doi.org/10.1016/s0166-4328(02)00026-8).

Martínez-Cué, C., Rueda, N., García, E., Davisson, M.T., Schmidt, C., Flórez, J., 2005. Behavioral, cognitive and biochemical responses to different environmental conditions in male Ts65Dn mice, a model of Down syndrome. *Behav. Brain Res.* 163, 174–185. <https://doi.org/10.1016/j.bbr.2005.04.016>.

McShane, B.B., Galante, R.J., Biber, M., Jensen, S.T., Wyner, A.J., Pack, A.I., 2012. Assessing REM sleep in mice using video data. *Sleep* 35, 433–442. <https://doi.org/10.5665/sleep.1712>.

Mesa-Gresa, P., Pérez-Martínez, A., Redolat, R., 2013. Environmental enrichment improves novel object recognition and enhances agonistic behavior in male mice. *Aggress. Behav.* 39, 269–279. <https://doi.org/10.1002/ab.21481>.

Morici, F.J., Bekinschtein, P., Weisstaub, N.V., 2015. Medial prefrontal cortex role in recognition memory in rodents. *Behav. Brain Res.* 292, 241–251.

Nithianantharajah, J., Hannan, A.J., 2006. Enriched environments, experience-dependent plasticity and disorders of the nervous system. *Nat. Rev. Neurosci.* 7, 697–709. <https://doi.org/10.1038/nrn1970>.

Nolte, G., Ziehe, A., Nikulin, V.V., Schlögl, A., Krämer, N., Brismar, T., Müller, K.-R., 2008. Robustly estimating the flow direction of information in complex physical systems. *Phys. Rev. Lett.* 100, 234101. <https://doi.org/10.1103/PhysRevLett.100.234101>.

Pons-espinal, M., Lagran, M.M.D., Dierssen, M., 2013. Environmental enrichment rescues DYRK1A activity and hippocampal adult neurogenesis in TgDyrk1A. *Neurobiol. Dis.* 60, 18–31. <https://doi.org/10.1016/j.nbd.2013.08.008>.

Puig, M.V., Alemany-González, M., Gener, T., 2020. Data for prefrontal-hippocampal functional connectivity encodes recognition memory and is impaired in intellectual disability 1. <https://doi.org/10.17632/wg4zm32gsb.1>.

Pujol, J., del Hoyo, L., Blanco-Hinojo, L., de Sola, S., Macià, D., Martínez-Vilavella, G., Amor, M., Deus, J., Rodríguez, J., Farré, M., Dierssen, M., de la Torre, R., 2015. Anomalous brain functional connectivity contributing to poor adaptive behavior in Down syndrome. *Cortex* 64, 148–156. <https://doi.org/10.1016/j.cortex.2014.10.012>.

Ramírez-Toráño, F., García-Alba, J., Bruña, R., Esteba-Castillo, S., Vaquero, L., Pereda, E., Maestú, F., Fernández, A., 2021. Hypersynchronized magnetoencephalography brain networks in patients with mild cognitive impairment and Alzheimer's disease in Down syndrome. *Brain Connect.* <https://doi.org/10.1089/brain.2020.0897>.

Ramón-Duaso, C., Gener, T., Consegal, M., Fernández-Avilés, C., Gallego, J.J., Castarlenas, L., Swanson, M.S., de la Torre, R., Maldonado, R., Puig, M.V., Robledo, P., 2019. Methylphenidate attenuates the cognitive and mood alterations observed in Mbni2 knockout mice and reduces microglia overexpression. *Cereb. Cortex* 29, 2978–2997. <https://doi.org/10.1093/cercor/bhy164>.

Raveau, M., Polygalov, D., Boehringer, R., Amano, K., Yamakawa, K., Mchugh, T.J., 2018. Alterations of in vivo CA1 network activity in Dp(16)1Yey Down syndrome model mice. *Elife* 7, e31543. <https://doi.org/10.7554/elife.31543.001>.

Ruiz-Mejías, M., 2019. Outer brain oscillations in Down syndrome. *Front. Syst. Neurosci.* 13, 17. <https://doi.org/10.3389/fnsys.2019.00017>.

Scheffer-Teixeira, R., Tort, A.B.L., 2017. Unveiling fast field oscillations through comodulation. *eNeuro*. <https://doi.org/10.1523/ENEURO.0079-17.2017>, 4: ENEURO.0079-17.2017.

Shinohara, Y., Hosoya, A., Hirase, H., 2013. Experience enhances gamma oscillations and interhemispheric asymmetry in the hippocampus. *Nat. Commun.* 4 <https://doi.org/10.1038/ncomms2658>.

Sohal, V.S., Rubenstein, J.L.R., 2019. Excitation-inhibition balance as a framework for investigating mechanisms in neuropsychiatric disorders. *Mol. Psychiatry* 24, 1248–1257. <https://doi.org/10.1038/s41380-019-0426-0>.

Spanswick, S.C., Dyck, R.H., 2012. Object/context specific memory deficits following medial frontal cortex damage in mice. *PLoS One* 7, e43698. <https://doi.org/10.1371/journal.pone.0043698>.

Steriade, M., 2006. Grouping of brain rhythms in corticothalamic systems. *Neuroscience* 137, 1087–1106. <https://doi.org/10.1016/j.neuroscience.2005.10.029>.

Tanaka, M., Wang, X., Mikoshiba, K., Hirase, H., Shinohara, Y., 2017. Rearing-environment-dependent hippocampal local field potential differences in wild-type and inositol trisphosphate receptor type 2 knockout mice. *J. Physiol.* 595, 6557–6568. <https://doi.org/10.1113/JP274573>.

Tort, A.B.L., Komorowski, R., Eichenbaum, H., Kopell, N., 2010. Measuring phase-amplitude coupling between neuronal oscillations of different frequencies. *J. Neurophysiol.* 104, 1195–1210. <https://doi.org/10.1152/jn.00106.2010>.

Valbuena, S., García, A., Mazier, W., Paternain, A.V., Lerma, J., 2021. Unbalanced dendritic inhibition of CA1 neurons drives spatial-memory deficits in the Ts2Cje Down syndrome model. *Nat. Commun.* 10, 4991. <https://doi.org/10.1038/s41467-019-13004-9>.

Valero, M., Averkin, R.G., Fernandez-lamo, I., Cid, E., Tamas, G., Valero, M., Averkin, R.G., Fernandez-lamo, I., Aguilera, J., Lopez-pigozzi, D., Brotons-mas, J.R., Cid, E., Tamas, G., Menendez de la Prida, L., 2017. Mechanisms for selective single-cell reactivation during offline sharp-wave ripples and their distortion by fast ripples. *Neuron* 94, 1234–1247.e7. <https://doi.org/10.1016/j.neuron.2017.05.032>.

van Praag, H., Kempermann, G., Gage, F.H., 2000. Neural consequences of environmental enrichment. *Nat. Rev. Neurosci.* 1, 191–198. <https://doi.org/10.1038/35044558>.

Velikova, S., Magnani, G., Arcari, C., Falautano, M., Franceschi, M., Comi, G., Leocani, L., 2011. Cognitive impairment and EEG background activity in adults with Down's syndrome: a topographic study. *Hum. Brain Mapp.* 32, 716–729. <https://doi.org/10.1002/hbm.21061>.

Wang, H., Xu Xiaxia, Xu, Xinxin, Gao J., Zhang, T., 2020. Enriched environment and social isolation affect cognition ability via altering excitatory and inhibitory synaptic density in mice hippocampus. *Neurochem. Res.* 45, 2417–2432. <https://doi.org/10.1007/s11064-020-03102-2>.

Wang, C., Furlong, T.M., Stratton, P.G., Lee, C.C.Y., Xu, L., Merlin, S., Nolan, C., Arabzadeh, E., Marek, R., Sah, P., 2021. Hippocampus–prefrontal coupling regulates recognition memory for novelty discrimination. *J. Neurosci.* 41, 9617–9632. <https://doi.org/10.1523/JNEUROSCI.1202-21.2021>.

Warburton, E.C., Brown, M.W., 2015. Neural circuitry for rat recognition memory. *Behav. Brain Res.* 285, 131–139. <https://doi.org/10.1016/j.bbr.2014.09.050>.

Yizhar, O., Fenno, L.E., Prigge, M., Schneider, F., Davidson, T.J., O'Shea, D.J., Sohal, V., S., Goshen, I., Finkelstein, J., Paz, J.T., Stehfest, K., Fudim, R., Ramakrishnan, C., Huguenard, J.R., Hegemann, P., Deisseroth, K., 2011. Neocortical excitation/inhibition balance in information processing and social dysfunction. *Nature* 477, 171–178. <https://doi.org/10.1038/nature10360>.